Ionic Transport, Reaction Kinetics, and Gel Formation. A Low-Field Overhauser Magnetic Resonance Imaging Study

Wilson Barros, Jr. and M. Engelsberg*

Departamento de Física, Universidade Federal de Pernambuco, 50670-901 Recife, Pernambuco, Brazil

Received: March 4, 2002; In Final Form: May 15, 2002

The electronic Overhauser effect was employed to enhance nuclear magnetic resonance images obtained in a magnetic field of only 16 mT. Despite the weak magnetic field, the technique can reveal, in some systems, various aspects of ionic transport and kinetics apparently not observed in conventional high-field magnetic resonance imaging. We employed Overhauser imaging to monitor the spatial and temporal evolution of the gelation of sodium alginate by calcium ions. The sensitivity of the Overhauser enhancement to small changes in gel composition permits a stringent test of the underlying mechanisms of transport and chemical kinetics.

I. Introduction

Transport of reacting ionic species in the presence of a concentration gradient is a ubiquitous phenomenon present in many chemical and biological processes. If two initially separated ionic species are placed in contact and a reaction takes place, the reacted interface may sometimes act as a virtual membrane with different transit times for ions of the two species. As a consequence, induced electric fields[1,2] may play an important role in ionic transport. The ensuing spatial and temporal evolution could be controlled not only by the diffusion coefficients and the reaction rates but also by the locally induced electric fields. Monitoring in a quantitative manner the spatial and temporal evolution of such processes may provide important clues of the underlying mechanisms of transport and of chemical kinetics.

In this work, we employ Overhauser magnetic resonance imaging in a low magnetic field to probe the spatial and temporal evolution of two reacting ionic species by monitoring their reaction product. The gelation of sodium alginate by calcium ions is a process that involves some of the aspects mentioned earlier and has inherent interest in various practical applications. Polysaccharides such as sodium alginate are being employed with increasing frequency for gel entrapment of living cells,[3,4] implants,[5] and other applications.[6] Sodium alginate is especially interesting for its ability to form, with divalent cations such as calcium, a lattice of cross-linked chains that provides a biologically mild environment for immobilization of living cells.

Despite the complexity of this problem, mathematical models have been proposed[7,8] aiming at a simplified description of the gelation process and the effective parameters controlling it. Because, for many applications, it is important to control the spatial heterogeneity of the gel, a prediction of the composition of the final gel distribution for simple geometrical shapes and its dependence upon operational parameters is expected to be quite useful. For immobilization of living cells, for example, a high gel concentration is generally required at the boundary to provide good mechanical strength, while a low gel concentration is necessary at the center for optimum biochemical activity.

* To whom correspondence should be addressed. E-mail: mario@df.ufpe.br.

Magnetic resonance imaging (MRI) has proven to be a powerful tool for monitoring the evolution of processes involving transport under the effect of a gradient of an external parameter, such as pressure, concentration, or chemical composition.[9−13] High-field (2 T) conventional proton MRI has been employed earlier in a study of the gelation process of sodium alginate,[13] but the analysis was limited to the time evolution of the sol−gel interface rather than the full gelation profile. Unlike conventional MRI, proton−electron double resonance imaging (PEDRI),[14−17] using the electronic Overhauser effect, is especially powerful at low magnetic fields. In this case, the electronic Larmor frequency can be maintained sufficiently low and a good penetration of the irradiation field is possible for samples of practical size. The use of such low magnetic fields may also have significant consequences from an instrumentation point of view, given the simplicity of the magnet required.

Newly developed free radicals of the trityl family[18,19] provide a source of electron spins that permits a large Overhauser enhancement with relatively small irradiation field strength. Moreover, the sensitivity of the Overhauser enhancement to small variations in gel composition[20] permits the observation of effects not previously reported in conventional MRI studies.

We here present the result of measurements of calcium alginate gelation profiles as a function of time under various conditions in samples with a cylindrical symmetry. These data permit a more detailed study of the transport and reaction kinetics than earlier MRI data. The results are compared with predictions of a recently proposed model constituting a stringent test of the validity of various assumptions connected to the kinetics and transport mechanisms in this system.

II. Experimental Results

PEDRI measurements in a magnetic field of only 16 mT were performed in a home-built system[21] operating at a proton Larmor frequency of 680 kHz. As a source of unpaired electron spins for the electronic Overhauser effect, the recently developed trityl free radical OX063[18] was employed. The electron spin resonance line of this radical, with a Larmor frequency of 447 MHz, is not split by hyperfine interactions as in nitroxide radicals and is also very narrow.[19,22] As a consequence, a quite large

10.1021/jp025718a CCC: $22.00 © 2002 American Chemical Society
Published on Web 07/12/2002

enhancement can be achieved with moderately low irradiation power.

The experimental arrangement employed was somewhat similar to the one used by Potter et al.[13] in their high-field MRI study. A cylindrical dialysis membrane, impermeable to the polysaccharide but permeable to other ions, was employed. With an internal diameter $2b = 14.5$ mm and a height of 25 mm, the membrane was surrounded by a cylindrical glass vial with internal diameter $2B = 25$ mm forming two concentric reservoirs. The external reservoir contained a 0.06 M solution of $CaCl_2$, and the internal reservoir contained an aqueous solution of sodium alginate. In both reservoirs, dissolved trityl OX063 free radical was present at a 2.5 mM concentration.

The two concentric sample holders were placed inside an inductively coupled birdcage resonator, approximately 3 cm in diameter, tuned to the electronic Larmor frequency. The cylindrical resonator produced quite a uniform radio frequency magnetic field in the region of interest, but in the region of the external $CaCl_2$ reservoir, spatial field inhomogeneity was observable for some range of azimuthal angles.[20] The resonator and the sample holders were positioned at the center of the NMR receiver coil and placed inside the horizontal magnet bore.

Data were acquired using a conventional spin−echo imaging sequence in a PEDRI mode.[16] The echo time was TE = 30 ms, and the recycling time of the spin−echo sequence was TR = 1.8 s. Preceding the spin−echo sequence, within the TR interval, a 500 ms electronic irradiation pulse from a 10 W amplifier was inserted.

The gradient strengths were adjusted for an in-plane pixel size of 0.43 mm with a slice thickness of 20 mm. The acquisition time for each image was 7.7 min for a 64 × 64 matrix with four scans for signal averaging. The Overhauser enhancement in the region of the external reservoir was approximately 50 for a 2.5 mM concentration of the trityl radical OX063. This was determined by comparison with a reference sample located within the receiver coil but not Overhauser irradiated.

Once dialysis against the external $CaCl_2$ solution was started, PEDRI profiles of the gelation process were obtained at time intervals of approximately 30 min, up to a maximum of 270 min. The imaging time of 7.7 min provided acceptable time resolution and relatively little blurring due to spatial averaging of the slow transport process. Typical PEDRI signal profiles of the gelation process are shown in Figure 1 for an initial sodium alginate concentration in the inner reservoir of 3% (w/v) and an initial 0.06 M $CaCl_2$ concentration in the outer reservoir. Radial profiles for different azimuthal angles differed only slightly. It was found to be quite representative to plot profiles for those azimuths for which no radio frequency field inhomogeneity was detectable in the outer reservoir.. The amplitudes are in arbitrary units with the value 256 corresponding to the PEDRI signal amplitude in the region of the external reservoir.

The profiles shown in Figure 1 illustrate the sensitivity of the Overhauser enhancement to variations in gel composition[20] as the formation of bound calcium salt bridges progresses. In previous studies of this system using conventional MRI and other methods,[13,23] quantitative information about the transport process was obtained by monitoring the spatial displacement of a gelation front at the sol−gel interface. In an effectively one-dimensional configuration and for a very fast reaction rate, the calcium diffusion coefficient at the interface has been correlated with the displacement of the gelation front.[13,7] Given that the purpose of this study is to take full advantage of all of the information contained in PEDRI data such as those of Figure 1, it becomes necessary to translate the signal profiles of Figure 1 into bound calcium profiles to test realistic models of the process. This requirement could be avoided if what is sought is only the time evolution of the interface, provided it is sharply defined. The data of Figure 1 indicate that, although a well-defined transition can actually be observed in some of the Overhauser images,[20] the bound calcium profiles exhibit a generally gradual spatial variation.

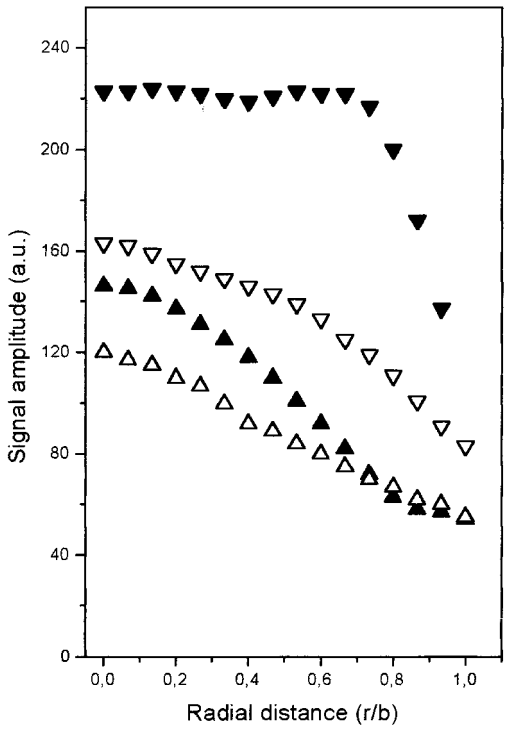

Figure 1. PEDRI signal amplitude profiles plotted against the relative radial distance from the center for an initial sodium alginate concentration of 3% (w/v) and an initial 60 mM Ca^{2+} concentration in the external reservoir. The signal profiles correspond to reaction times (△) $t = 270$ min, (▲) $t = 210$ min, (▽) $t = 120$ min, and (▼) $t = 15$ min. The trityl radical concentration was 2.5 mM.

To convert signal profiles into bound calcium profiles, calibration curves became necessary. The main assumption is that the spatial evolution of the gelling process does not significantly alter the local degree of water mobility with respect to static homogeneous conditions for the same concentration of bound calcium. Furthermore, the reactivity is known to be negligible for the chemical species involved. Hence, a uniform distribution of elecronic spins may be assumed on the spatial scale of the experiment.

The calibration procedure involved the same arrangement of two concentric reservoirs but with a glass partition substituting for the dialysis membrane. The external reservoir, still containing a 0.06 M $CaCl_2$ solution and a 2.5 mM concentration of radical, served as a signal reference for the Overhauser enhancement. For the actual calibration, we used the signal intensity from the inner reservoir, which contained various spatially uniform control gels with a range of calcium concentrations and a given initial concentration of sodium alginate. For reliable results, these control samples were required to be spatially homogeneous on a scale smaller than a pixel size. Because the reaction is quite fast, simply vigorously stirring a known amount of $CaCl_2$ solution into a sodium alginate solution containing the free radical was only found to be adequate for small calcium concentrations. To circumvent this difficulty we employed, for larger calcium concentrations, the procedure proposed by Draget et al.,[24] whereby a fine dispersion of insoluble $CaCO_3$, together

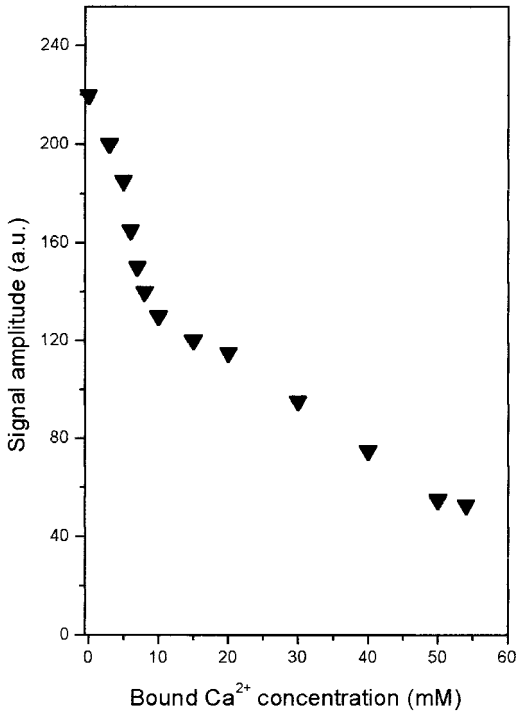

Figure 2. PEDRI signal amplitude as a function of bound Ca^{2+} concentration in spatially uniform alginate control gels. The sodium alginate concentration was 3% (w/v), and the trityl radical concentration was 2.5 mM.

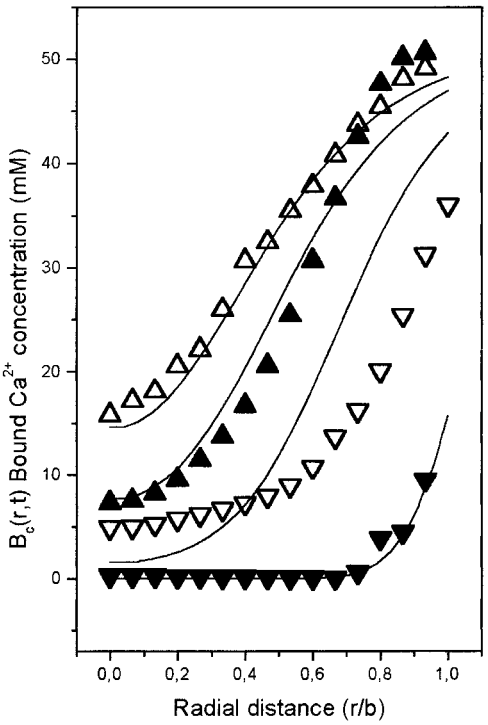

Figure 3. Bound Ca^{2+} profiles, $B_c(r,t)$, plotted against relative radial distance from the center for a 3% (w/v) initial sodium alginate concentration, 2.5 mM trityl radical concentration, and 60 mM initial Ca^{2+} concentration in the external reservoir. The profiles correspond to reaction times (△) $t = 270$ min, (▲) $t = 210$ min, (▽) $t = 120$ min, and (▼) $t = 15$ min. The solid lines represent calculated bound Ca^{2+} profiles.

with a hydrolyzing agent (δ-gluconolactone), permits a slow conversion to dissolved calcium ions yielding very homogeneous gels. As a check, this latter procedure yielded, for low calcium concentrations, results that were found to be compatible with the direct calibration using a $CaCl_2$ solution.

Figure 2 shows a calibration curve for 3% (w/v) sodium alginate with the horizontal axis representing bound calcium molarity in the control gel and the vertical axis representing the corresponding PEDRI signal amplitude at a 2.5 mM concentration of radical. The amplitude assigned to the signal from the external reservoir was 256.

PEDRI signal amplitude not only is a function of calcium concentration in the gel but also depends on the initial sodium alginate concentration. Thus, different calibration curves are needed to convert the signal amplitude when the initial sodium alginate concentrations are different from that of Figure 2. To the extent that alginate diffusion can be considered to have a negligible effect during the time of the dialysis experiment, the use of calibration curves such as that of Figure 2, but with a different sodium alginate concentration, can be expected to be applicable to an actual dialysis experiment in which this new initial sodium alginate concentration prevails.

A characteristic of hydrogels is that, even though the macroscopic viscosity diverges at the gel point, water molecules still remain quite mobile. Thus, the Overhauser enhancement, sensitive to the fluctuations in electron−nucleus dipole−dipole interaction,[25] drops very rapidly as the macroscopic viscosity increases and the gel point is approached. However, the drop still continues, at a slower rate, until a limit is reached for larger calcium concentrations.

The calibration curve of Figure 2 quantitatively demonstrates the sensitivity of the Overhauser enhancement to changes in calcium concentration. The initial signal amplitude, for 3% (w/v) sodium alginate, can be seen to be somewhat lower than the reference value 256. This is expected from the larger viscosity of the alginate solution compared to the aqueous $CaCl_2$ reference solution. A drop in signal amplitude by approximately a factor of 2 takes place when the calcium concentration in the gel increases to approximately 10 mM. Within this range, concentration variations of less than 1 mM can be detected and the large sensitivity of the Overhauser effect becomes most apparent. For larger calcium concentrations, the signal amplitude drops at a slower rate and reaches a steady-state value for a calcium concentration of approximately 53 mM. Assuming stoichiometric formation of salt bridges at this steady-state value, 1 g of our commercial sodium alginate would correspond to 0.0036 mol of guluronic carboxyl units. This is in very good agreement with the value reported by Potter et al.[13] The overall signal changes by a factor of approximately 5.0 for a 3% (w/v) initial sodium alginate concentration and TE = 30 ms. This permits the observation of small variations in signal profiles, especially for low calcium concentrations.

Figure 3 shows bound calcium profiles obtained from the signal profiles of Figure 1 by a polynomial interpolation from the calibration curve in Figure 2. A striking result, not apparent from previous conventional MRI,[13] is the presence of an unexpectedly sizable concentration of bound calcium at the center of the cylinder for very short times. This observation will be seen to be an important clue for a realistic description of the transport process and the kinetics.

III. Discussion

The results of section II can be employed for a quantitative test of the underlying mechanisms of transport and kinetics. Mikkelsen et al.[8] proposed a model in which the space and time evolutions of the gelation process were assumed to be describable, as a first approximation, by three space- and time-

dependent quantities: the concentration of alginate monomer chains $a(r,t)$, measured by the total number of moles of carboxyl groups (repeating units), the free calcium molar concentration $c(r,t)$, and the gel concentration $g(r,t)$. This last quantity represents the concentration of n-mers ($n \geq 2$) formed by calcium salt bridges also measured by the total number of moles of carboxyl repeating units. We have assumed cylindrical symmetry, with r denoting the radial distance to the center of the cylinder.

The space and time evolutions were further assumed to be governed by diffusion and by an irreversible chemical reaction according to the following set of coupled partial differential equations:

$$\frac{\partial c}{\partial t} = D_c \nabla^2 c - k\bar{N}_c c a^2 - k\bar{N}_c c a g \quad (1)$$

$$\frac{\partial a}{\partial t} = \nabla(D_a \nabla a) - k c a^2 - k c a g \quad (2)$$

$$\frac{\partial g}{\partial t} = k c a^2 + k c a g \quad (3)$$

D_c in eqs 1−3 denotes the free calcium diffusion coefficient, assumed to be constant, and D_a represents the free alginate diffusion coefficient, which may depend on $a(r,t)$ and $g(r,t)$. For simplicity, a single reaction rate k, corresponding to the formation of alginate n-mers ($n \geq 2$), was assumed. Electrostatic effects were neglected, as well as the diffusion of n-mers ($n \geq 2$).

In addition to the diffusion coefficients and the single reaction rate, eqs 1−3 contain another parameter, represented by $\bar{N}_c$, which is related to a basic assumption of the model concerning the kinetics of the gelation process. Although eq 1 is of first order in the free calcium concentration, it was assumed that the average number of calcium ions bound to each alginate n-mer ($n \geq 2$), denoted by $\bar{N}_c$, is larger than one. This postulate implies a highly cooperative process. The first alginate−Ca^{2+} binding immediately initiates the formation of a dimer bond by subsequent cooperative binding of additional Ca^{2+}, without any additional alginate molecules. Examples of this type of binding are found, for example, in the nucleation kinetics of nucleotides.[27] Moreover, to reproduce typical concentrations of calcium ions bound in the gel, large values of $\bar{N}_c$, typically 50 or even larger, would be needed. Such large values of $\bar{N}_c$ have a pronounced effect upon the gel profiles predicted by eqs 1−3, greatly hindering gel formation at the center of the cylinder.

We solved eqs 1−3 numerically[8] to assess to what extent $g(r,t)$ could describe the variations of bound calcium observed in our experiments. Using accepted estimates[8] for D_a, D_c, and k, we found that values of $\bar{N}_c$ as large as 50 were completely untenable for the time scale of our experiments. They predict, for reaction times such as that in Figure 3, very inhomogeneous gels with bound calcium concentrations at the center cylinder that are orders of magnitude smaller than those at the edge. This is contrary to the inhomogeneity apparent from Figure 3. Given the large sensitivity of the Overhauser enhancement to small changes of bound calcium concentration near the center of the cylinder, the values shown in Figure 3 can be considered reliable.

In reality, if the gel inhomogeneity predicted by eqs 1−3 is required to approach the experimental values shown in Figure 3, the value of $\bar{N}_c$ must be chosen to be close to unity, as required by stoichiometry. This requires a reinterpretation of the quantities defined therein. Because the collective binding effect must be abandoned, at least for our relatively short-time reaction regime, we are forced to adopt a standard kinetic approach. Hence, $a(r,t)$ is now interpreted not as a concentration of monomeric chains but rather as the actual molar concentration of nonbridged guluronic[8] carboxylic groups. Similarly, $g(r,t)$ is interpreted as the actual molar concentration of guluronic carboxylic groups associated in bound calcium bridges. Given this new interpretation, the two terms on the right-hand side of eq 1, representing the Ca^{2+} depletion rate caused by chemical reaction, must be combined into a single term $2kca^2$. Similarly, the twice as fast rate of chemical depletion of nonbridged guluronic carboxylic groups in eq 2, and the rate of increase of bridged carboxylic groups in eq 3, become simply $4kca^2$ in both equations.

Despite the many simplifications implicit in this model, it is quite instructive to compare its predictions with the data of Figure 3. The coupled set of modified differential equations was solved numerically[8] in cylindrical coordinates for the dimensionless quantities $G(r,t) = g(r,t)/a(0)$, $A(r,t) = a(r,t)/a(0)$, and $C(r,t) = c(r,t)/a(0)$, where the constant $a(0) = 0.106$ M denotes the initial molar concentration of guluronic carboxylic groups in the 3% (w/v) sodium alginate solution. The molar concentration of bound calcium plotted in Figure 3 is now expected to be simply given by the stoichiometric relationship $B_c(r,t) = G(r,t)a(0)/2$.

Because the volume of the external reservoir in our experiment is only a factor of 2 larger than that of the inner reservoir, the depletion of Ca^{2+} in the external reservoir during the reaction times of Figure 3 had to be taken into account. This was accomplished through a suitable boundary condition at the dialysis membrane.[8] Furthermore, assuming for the repeating[28] alginate macromolecules a very small diffusion coefficient, typically of the order $10^{-3}D_c$,[8] the effect upon the calculated bound Ca^{2+} profiles was found to be negligible, at least for relatively short times such those in Figure 3. Thus, only two adjustable parameters, an effective calcium diffusion coefficient D_c and an effective reaction rate k, would be required for a comparison with the data of Figure 3.

Figure 3 shows calculated bound Ca^{2+} profiles obtained from the modified eqs 1−3 for various reaction times. Given that the experimental profiles for times less than approximately 200 min significantly depart from the parabolic-like shape characteristic of Fickian diffusion, we chose to adjust the two parameters so that $B_c(r,t)$ yields the best possible fit for times longer than 200 min. The calculated profiles for $t = 270$ min and $t = 210$ min shown in Figure 3, which appear to be in fairly good agreement with the data, correspond to a value of the effective reaction rate of $k = 3 \times 10^{-2}$ M^{-2} sec^{-1}. This value is not incompatible with other approximate estimates that have been reported for this quantity.[8]

The effective Ca^{2+} diffusion coefficient, $D_c = 0.81 \times 10^{-5}$ cm^2/sec, obtained from the fits of Figure 3 deserves special attention. This value almost coincides with 0.79×10^{-5} cm^2/sec, the free Ca^{2+} diffusion coefficient at infinite dilution.[29] From this result, one is led to conclude that Ca^{2+} transport through the gel is, somewhat unexpectedly, as efficient as in aqueous solution under optimum conditions. This enhanced transport becomes more evident if one examines the shorter time behavior. A comparison between the experimental profile for $t = 120$ min and the calculated profile shows significant discrepancies. Even with such a large value of D_c, the measured concentration of bound Ca^{2+} at the center appears to be almost a factor of 3 larger than the predicted value. Furthermore, the shape of the profile departs considerably from the theoretical prediction

resembling profiles in which collective flow competes with pure diffusion.[21,30,31]

The source of these discrepancies can be attributed to electrostatic effects not included in eqs 1−3. The presence of such effects in the present system was readily verified by inserting platinum electrodes and monitoring the voltage as the gelation progressed. The large difference in transit times across the dialysis membrane, especially between the anions, induces an electric field directed toward the center. This causes a bulk transport of Ca^{2+} with a quite pronounced flow at the beginning of the process. Moreover, as the network of cross-linked chains grows, enlarging the size of the effective membrane, the collective motion changes to a regime that may be characterized as effectively diffusive, albeit with a larger apparent diffusion constant.

A more realistic approach to this problem should involve the numerical solution of the complete Nernst−Planck and Poisson equations.[1,32] This includes all ions and their diffusion coefficients in the dialysis membrane as well as in the gel. Equation 1 for the free Ca^{2+} concentration $c(\vec{r},t)$, for example, should be complemented by an additional term of form[1,32] $-D_c\nabla[2c(\vec{r},t)(F/(RT))\vec{E}(\vec{r},t)]$, where F, R, and T denote, respectively, Faraday's constant, the gas constant, and absolute temperature. The induced electric field, $\vec{E}(\vec{r},t)$, is further determined self-consistently by a Poisson equation involving all ions. Although a full solution of these equations will not be attempted here, some qualitative arguments could be useful. If a regime were reached in which the induced electric field approaches the simple form $\vec{E} = -\Gamma(\nabla c)/c$, with Γ denoting a positive constant, an effectively diffusive process would be established. Such a spatial and temporal dependence of the electric field would lead to Fickian profiles, as in Figure 3 for $t = 210$ and 270 min. However, an apparent diffusion coefficient larger than the pure self-diffusion coefficient by a factor $1 + 2\Gamma F/(RT)$ would have to be invoked.

An estimate of Γ is possible from the data of Figure 3 for $t = 210$ and $t = 270$ min. Assuming for the true Ca^{2+} diffusion coefficient the value 0.3×10^{-5} cm^2/sec, determined by Potter et al.,[13] and 0.81×10^{-5} cm^2/sec for the apparent diffusion coefficient, one obtains $\Gamma = 22$ mV, which is not inconsistent with typical values for this system.

IV. Conclusions

We conclude that Overhauser imaging in very low magnetic fields may be a powerful tool to study processes involving transport and chemical reaction via actual concentration profiles. This may include processes involving chemical waves and other spatio-temporal phenomena.[33] Not only new effects may become accessible but also the magnet design and cost become much more affordable.

The study of bound Ca^{2+} gelation profiles in sodium alginate cross-linked by Ca^{2+} ions was found to furnish a good example of the possibilities permitted by this technique. Thanks to the large sensitivity of the Overhauser enhancement to small changes in bound Ca^{2+} during the initial phase of the process, new aspects, apparently not observed in earlier conventional MRI, could be examined. A proposed cooperative effect in the kinetics of alginate gel formation was found to be inconsistent with our experimental results. The proposed effect, which provides an explanation for the steady-state gel compositions at long times,[8] was found to be incompatible with our results for the initial stages of the process. The transport of Ca^{2+} through the forming gel was found to be significantly enhanced by electrostatic effects.[34] Moreover, the shapes of the profiles, especially in the initial phase, appear to be strongly affected by bulk flow caused by the induced electric fields.

Acknowledgment. We thank Dr. Klaes Golman and Dr. J. H. Ardenkjaer-Larsen of Nycomed Innovation AB for making available the trityl radical OX063. We also thank Fernando Hallwass and Humberto Vasconcelos Beltrão Neto for able assistance. This work was supported by Conselho Nacional de Desenvolvimento Científico e Tecnológico (Brazilian agency).

References and Notes

(1) Nernst, W. *Z. Phys. Chem.* **1888**, *2*, 613. Nernst, W. *Z. Phys. Chem.* **1889**, *4*, 129.
(2) Planck, M. *Ann. Phys. Chem.* **1890**, *39*, 161. Planck, M. *Ann. Phys. Chem.* **1890**, *40*, 561.
(3) Vorlop, K. D.; Klein, J. *Enzyme Technology*; Springer-Verlag: Berlin, 1983.
(4) Mattiasson, B. In *Immobilized Cells and Organelles*; Mattiesson, B., Ed., CRC Press: Boca Raton, FL, 1983; Vol. 1.
(5) Shiong, P. S.; Feldman, E.; Nelson, R.; Heintz, R.; Yao, Q.; Yao, Z.; Zheng, T.; Merideth, N.; Bræk, G. S.; Espevik, T.; Smidsrød, O.; Sandford, P. *Proc. Natl. Acad. Sci. U.S.A.* **1993**, *98*, 5843.
(6) Smidsrød, O.; Bræk, G. S. *Trends Biotechnol*. **1990**, *8*, 71.
(7) Sherwood, T. K.; Pigford, R. L. *Absorption and Extraction*, 2nd ed.; McGraw-Hill: New York, 1952.
(8) Mikkelsen, A.; Elgsaeter, A. *Biopolymers* **1995**, *36*, 17.
(9) Gummerson, R. J.; Hall, C.; Hoff, W. D.; Hawkes, R.; Holland, G. N.; Moore, W. S. *Nature (London)* **1979**, *281*, 56.
(10) Blackband, S.; Mansfield, P. *J. Phys. C* **1986**, *19*, L49.
(11) Mansfield, P.; Bowtell, R.; Blackband, S. *J. Magn. Reson.* **1992**, *99*, 507.
(12) Schrader, G. W.; Litchfield, J. B. *Drying Technol.* **1992**, *10*, 295.
(13) Potter, K.; Balcom, B. J.; Carpenter, T. A.; Hall, L. D. *Carbohydr. Res*. **1994**, *257*, 117.
(14) Overhauser, A. W. *Phys. Rev.* **1953**, *92*, 411.
(15) Warmuth, W. M.; Kramer, K. D. *Z. Naturforsch*. **1964**, *19a*, 375.
(16) Lurie, D. J.; Bussell, D. M.; Bell, L. H.; Mallard, J. R. *J. Magn. Reson*. **1988**, *76*, 366.
(17) Grucker, D. *Magn. Reson. Med*. **1990**, *14*, 147.
(18) Nycomed Innovation AB, Malmö, Sweden (proprietary compound).
(19) Larsen, J. H. A.; Laursen, I.; Leunbach, I.; Ehnholm, G.; Wistrand, L. G.; Petersson, J. S.; Golman, K. *J. Magn. Reson.* **1998**, *133*, 1.
(20) Barros Junior, W.; de Souza, R. E.; Engelsberg, M.; Golman, K.; Larsen, J. H. A. *Appl. Phys. Lett.* **2002**, *80*, 160.
(21) do Nascimento, G. C.; Engelsberg, M.; de Souza, R. E. *Meas. Sci. Technol*. **1992**, *3* (4), 370.
(22) Golman, K.; Leunbach, I.; Larsen, J. H. A.; Ehnholm, G. J.; Wistrand, L. G.; Petersson, J. S.; Järvi, A.; Vahasalo, S. *Acta Radiol*. **1998**, *39*, 10.
(23) Gudmund, S. B.; Grasdalen, H.; Smidsrød, O. *Carbohydr. Polym*. **1989**, *10*, 31.
(24) Draget, K. I.; Østgaard, K.; Smidsrød, O. *Carbohydr. Polym.* **1991**, *14*, 159.
(25) de Sousa, P. L.; de Souza, R. E.; Engelsberg, M.; Colnago, L. A. *J. Magn. Reson*. **1998**, *135*, 118.
(26) Wang, Z. Y.; Zhang, Q. Z.; Konno, M.; Saito, S. *Chem. Phys. Lett.* **1991**, *186*, 463.
(27) Dugaiczyk, A.; Boyer, H. W.; Goodman, M. *J. Mol. Biol.* **1975**, *96*, 171.
(28) de Gennes, P. G. *J. Chem. Phys.* **1971**, *55*, 572.
(29) Wang, J. H. *J. Am. Chem. Soc*. **1953**, *75*, 1769.
(30) de Sousa, P. L.; Engelsberg, M.; Moreira, F. G. B. *Phys. Rev. E* **1999**, *60*, R1174−1177.
(31) de Sousa, P. L.; Engelsberg, M. *Phys. Rev. E* **1999**, *60*, 7541.
(32) Sokalski, T.; Lewenstam, A. *Electrochem. Commun*. **2001**, *3*, 107.
(33) Epstein, I. R.; Showalter, K. *J. Phys. Chem.* **1996**, *100*, 13132.
(34) Hart, T. D.; Hill, R. J.; Glover, P. M.; Lynch, J. M.; Chamberlain, A. H. L. *Enzyme Microb. Technol.* **2001**, *28*, 370.